Journal of Marine Science and Technology

Volume 25 | Issue 6 Article 2

MODIFIED PID CONTROLLER DESIGN FOR ACTIVE TRANSVERSE ANTI-ROLLING SYSTEM FOR SHIPS WITH LOW ROLL MOTION

Hsing-Cheng Yu
Department of Systems Engineering and Naval Architecture, National Taiwan Ocean University, Keelung, Taiwan, R.O.C., hcyu@ntou.edu.tw

Jhih-Jyun You
Department of Systems Engineering and Naval Architecture, National Taiwan Ocean University, Keelung, Taiwan, R.O.C.

Recommended Citation
Yu, Hsing-Cheng and You, Jhih-Jyun (2017) "MODIFIED PID CONTROLLER DESIGN FOR ACTIVE TRANSVERSE ANTI-ROLLING SYSTEM FOR SHIPS WITH LOW ROLL MOTION," *Journal of Marine Science and Technology*: Vol. 25: Iss. 6, Article 2.
DOI: 10.6119/JMST-017-1226-02
Available at: https://jmstt.ntou.edu.tw/journal/vol25/iss6/2

Journal of Marine Science and Technology, Vol. 25, No. 6, pp. 633-639 (2017)
DOI: 10.6119/JMST-017-1226-02

MODIFIED PID CONTROLLER DESIGN FOR ACTIVE TRANSVERSE ANTI-ROLLING SYSTEM FOR SHIPS WITH LOW ROLL MOTION

Hsing-Cheng Yu and Jhih-Jyun You

Key words: anti-rolling, modified PID control, ship, stabilizer fin.

ABSTRACT

Multi-domain physical modeling software with an intuitive simulation methodology using MapleSim was adopted in this study to create a rigid body structure model of an active transverse anti-rolling system (ATARS) of a container ship. At the same time, a ship stability analysis was also conducted to determine the force model, dynamic equilibrium, and motion behavior of the ATARS of the container ship. Once various external transverse force generated by waves impact varied roll angles of the ATARS on the vessel, a modified proportional-integral-derivative (PID) controller designed to improve the capability of the active stabilizer fins used in the ATARS is applied to reduce the roll angle. Consequently, using the modified PID controller, the maximum overshoot, roll angle, and steady-state error of the designed container ship were determined to be 11.2°, 340 s, and 6.1°, respectively.

I. INTRODUCTION

In general, ship stability deals with ship behavior at sea and affects the development of marine transportation. A ship sailing in a seaway is continuously affected by the wind and waves, and has six degrees of freedom motion, i.e., translation axes, i.e., or surge, sway, and heave; and rotation axes, which are the i.e., roll, pitch, and yaw (Zhao et al., 2014), as shown in Fig. 1.

Sailors and cargo on-board a ship will experience very heavy roll motion. Because the low damping coefficients of a ship can oppose the roll motion, the roll angles of the ship remain significant even in calm waves. When a larger roll angle occurs, it brings about a problem with regard to physical discomfort of the sailors and heavy damage to the cargo or instruments. Additionally, a roll angle with an over-load may overturn a ship. In addition to the roll angle, the consumption of oil and water also cause a free surface effect, to make thereby severely increasing the roll motion. Hence, this paper focuses on reducing the roll motion of a ship when at sea. In general, the ship dimensions, speed, and direction of the waves may affect the ship stability and motion. Larger dimensions or a faster speed are effective at reducing the roll motion. If the waves hit the side of the ship, it results in a roll motion. The safety while at sea is related to the changes in ship motion, especially roll motion (Robert, 1982). Anti-rolling systems can commonly be divided into two types: active and passive. According to the roll angle acquired by a motion sensor, an active anti-rolling system can adjust the righting moment to reduce the roll motion. The most commonly used active anti-rolling devices are active stabilizer fins, which are rectangle boards with a rudder-like shape, as shown in Fig. 2.

To generate righting moment to restrain the shaking, the angles

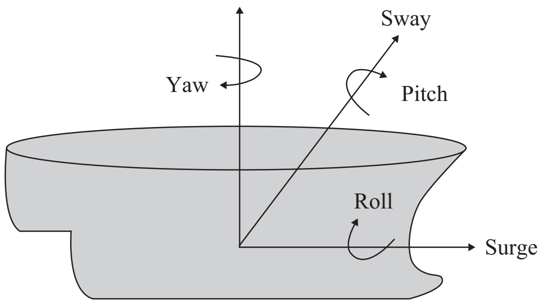

Fig. 1. Six degrees of freedom of a ship.

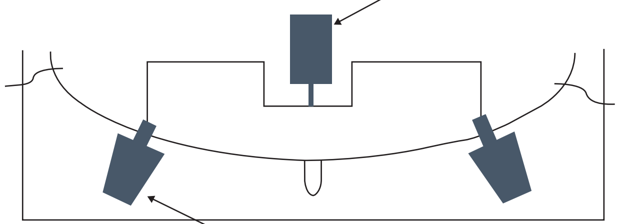

Fig. 2. Active stabilizer fins and control unit in an active anti-rolling system.

Paper submitted 06/14/17; revised 08/16/17; accepted 12/04/17. Author for correspondence: Hsing-Cheng Yu (e-mail: hcyu@ntou.edu.tw).
Department of Systems Engineering and Naval Architecture, National Taiwan Ocean University, Keelung, Taiwan, R.O.C.

between the foil and water flow need to be changed. A higher speed or larger contact area can be more efficient for reducing the roll motion of a vessel. Active stabilizer fins are usually applied to high-speed vessels, and the most active stabilizer fins are installed behind the bilge keel. Thus, this study presents the use of active stabilizer fins and a controller design to reduce roll motion.

II. ATARS AND PID CONTROLLER DESIGN

Anti-rolling systems can generally be divided into two types: active and passive. Passive anti-rolling systems include bilge keels, load repartition, anti-rolling tanks, and stabilizer fins. A bilge keel can adopt the resistance between itself and the water to reduce roll motion, is suitable for all ship dimensions. A bilge keel is also easy to maintain and is inexpensive. However, the influences of the ship velocity and roll motion need to be considered. This increases the resistance and decreases the efficiency. Load repartition is a method for arranging the cargo locations to reduce roll motion. Moreover, two types of anti-rolling tanks are allocated inside. In earlier years, people changed the weight of the water and oil tanks to modify the rolling periods; however, this easily leads to a free-surface effect and damages the stability of dynamic motion. Nowadays, to create the same effect, anti-rolling tanks are usually a U-shape using the moment produced by water, i.e., similar to a damper to reduce roll motion. Although they occupy a certain amount of space, they can be effective at any speed when the ship is at stall speed. Stabilizer fins extend from the ship body like the fins of a fish. The efficiency depends on the vessel speed, and is obvious at high speed and unclear at low speed (Kang et al., 2003).

An active anti-rolling system, also known as an active transverse anti-rolling system (ATARS), includes a gyroscopic system, a rudder anti-rolling system, an active anti-rolling tank, and active stabilizer fins. The gyroscopic system resists the roll motion through the moment produced by the rotational mass block. However, a concentrated mass may cause torque, thereby negatively influencing the ship structure and reducing the stability. It also incurs a high cost, and therefore few ships have such a device installed. An anti-rolling rudder system can cooperate with the engine power output. The moment produced can resist the roll motion and modify the angles of the rudders, but is useless at low speed. The greatest difference between active and passive anti-rolling tanks is the dampers or dynamic system that can be applied. The two types of tanks can change the water level differently to produce moment to resist the roll motion. In other words, they can make the systems controllable. Active stabilizer fins are able to change the angles of attack according to the different dynamic motions of the ship. They use the moment produced by the resistance to reduce the roll motion. Although they are affected by the speed, there is no efficiency loss at low speed, and they are therefore highly efficient devices.

1. Stabilizer Fins

Stabilizer fins are devices that extend from the ship's body, and are installed under water lines to produce lift by the angles between the foil and inflow to resist the roll motion and reduce roll angles. Lift (L) can be expressed as

$$L = \frac{1}{2} C_L \rho S V^2, \tag{1}$$

where C_L is the lift coefficient, ρ is the density of the sea water, S is the projected area of the foil, and V is the ship's velocity.

It can be seen from Eq. (1) that the lift is in direct proportion to the ship's velocity. The stabilizer fins will not work sufficiently if the ship is sailing at a low or stall speed. An active anti-rolling system has to have some sensors installed on ship to detect the dynamic motion of the ship. They can assist in modifying the attack angles of the stabilizer fins. Various angles of attack have different values of C_L to produce varied lift, which can improve their efficiency. The design condition of stabilizer fins has to allow the foil lift to produce sufficient moment to resist the roll torque produced by waves (Zhigang et al., 2015).

The design condition of a stabilizer fin is

$$2 \times \frac{1}{2} C_L \rho S V^2 r = \nabla \overline{GM} \phi, \tag{2}$$

where r is the length between the centers of gravity and the lift of the ship, ∇ is the displacement, $\overline{GM}$ is the height of meta center, and ϕ is the roll angle.

NACA0015, developed by the National Advisory Committee for Aeronautics (NACA), is adopted in this study for the design of a stabilizer fin. Its geometry can be realized based on defined model numbers. For a four-digit model, the first digit means the maximum camber percentage of the chord length. The second digit shows the ratio of the distance between the maximum camber and the leading edge to the chord length, which can be shown in one-tenth order. The last two digits indicate the maximum thickness of the chord length. It can be seen that NACA0015 is a symmetrical four-digit foil (Aziz et al., 2014).

The equation of half thickness for a symmetrical four-digit NACA foil is

$$y_t = 5tc \begin{bmatrix} 0.2969\sqrt{\frac{x}{c}} + (-0.1260)\left(\frac{x}{c}\right) + \ldots \\ (-0.3516)\left(\frac{x}{c}\right)^2 + 0.2843\left(\frac{x}{c}\right)^3 + \ldots \\ (-0.1015)\left(\frac{x}{c}\right)^4 \end{bmatrix}, \tag{3}$$

where c is the chord length, x is the position along the chord from 0 to c, y_t is the half the thickness at the given value of x, and t is the maximum thickness of the chord length. The foil can be calculated using Eq. (3), as illustrated in Fig. 3.

(a) cross section (b) perspective

Fig. 3. NACA0015.

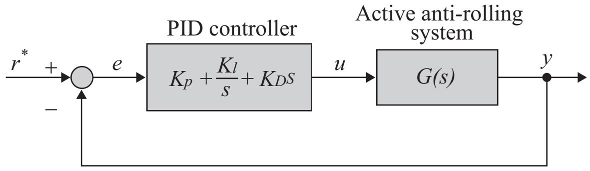

Fig. 4. System block diagram of ATARS with PID controller.

2. PID Controller Design

To reach the design requirements, the parameters of the controller need to be tuned. Proportional-integral-derivative (PID) control is the most common control method adopted in various applications. With advances in digital technology, most industrial controllers are implemented based around the PID algorithm. Hence, the popularity of PID control has grown tremendously (Ang et al., 2005). In addition, proportional-integral (PI) and proportional-derivative (PD) controllers can be considered as forms of phase-lag and phase-lead compensators, respectively. A PID controller can also be regarded as the form of a phase lead-lag compensator. A PID controller compares the feedback value with the reference value. It gains a difference between the feedback and the reference to be new output signal. The gain in terms of a PID controller includes three parts: a proportional term, an integral term, and a derivative term. There are three coefficients K_P, K_I, and K_D used in the model, which correspond to the error, past error, and possible future error, respectively. To tune the parameters of the controller, an experienced engineer is consulted or a trial and error method is generally used. A controller is mainly applied in linear and time-invariant systems, and can also be utilized in a system whose characteristics are unknown.

A system block diagram of a PID controller applied in an ATARS (Liang et al. 2009) is shown in Fig. 4.

In Fig. 4, r^* is the reference rolling input, e is the rolling error, u is the control effort voltage, y is the output of the ATARS, and $G(s)$ is the transfer function of the ATARS, in which the input is the roll angle of the ship, and the output is the driving voltage of an electric machine. During the simulation, the transfer function of $G(s)$ can be auto-identified using MapleSim. Once the simulated model is built, the dynamic response can be obtained through a simulation.

Because a PID controller is combined using a PI controller and PD controller, it can improve the relative stability of a closed-loop system, boost the transient response, and reduce the steady-state error. Control using a PID control algorithm in continuous time takes the form of

$$u(t) = K_P e(t) + K_I \int_0^t e(t)dt + K_D \frac{d}{dt}\left[e(t)\right] \tag{4}$$

where K_P, K_I, and K_D are the proportional, integral, and derivative gains, respectively, which are the tuning parameters of the PID controller. For the digital controller design, a discrete version of the PID control equation can be applied in continuous time. The difference between two points, one prior to sampling, and the other after sampling, is used to approximate the differential term. The gradient area and approximate integral term can be used to obtain the PID control theory in discrete time, as shown in Eq. (5).

$$\begin{aligned} u(k) &= K_P e(k) + K_I \sum_{i=0}^{k-1} e(i) + K_D\left[e(k) - e(k-1)\right] \\ &= K_P e(k) + \frac{K_P T_S}{T_I}\sum_{i=0}^{k-1} e(i) + \frac{K_P T_D}{T_S}\left[e(k) - e(k-1)\right] \end{aligned} \tag{5}$$

where T_S is the sampling time, T_I is the integral time constant, and T_D is the differential time constant.

The different parameters each have a different influence on the PID controller. The proportional controller can increase the response speed and improve the steady-state error slightly. The integral controller can improve the static error. The derivative controller is equal to a high-pass filter, and can improve the transient response. The influence of the parameters of the PID controller are shown in Table 1 (Zhong, 2011).

To tune the PID controller parameters effectively, there are many suitable methods. A manual adjustment, which is the most basic method, requires no specific tools but is less efficient. To improve the efficiency, a standard operational procedure needs to be established based on the dynamic characteristics of the system. The commonly used methods, i.e., trial and error, the Niegler-Nichols method (Niegler and Nichols, 1942), the Co hen-Coon method, and specific software, along with their benefits and drawbacks, are listed in Table 2.

The PID parameters must be tuned to achieve stability of the control system; however, such parameters are not always known. Datta et al. (2000) proposed a modified method that can guarantee the stability of the control system. However, a difficulty with the method remains in that the three parameters of the PID controller, i.e., K_P, K_I, and K_D, are related with each other. A control method for a multiple-input/multiple-output system was proposed by Hagiwara et al. (2010). In addition, not only can it specify the input-output characteristics and the disturbance attenuation characteristics separately, it can also decrease unknown disturbances (Hagiwara et al., 2010).

Table 1. The parameter influence of the PID controller design.

Gain-tuning \ Performance	Rise time	Over shoot	Control period	Steady-state error	System stability
K_P rise	decline	rise	rise	decline	worse
K_I rise	decline	rise	rise	decline	worse
K_D rise	decline	decline	decline	even	better

Table 2. Commonly used methods for tuning the PID controllers.

Methods \ Features	Benefit	Damage
Trial and error	Do not need mathematical mode	Need experience
Niegler-Nichols	Commonly useful	Parameters may make rapid response
Cohen-Coon	Good process model	Frist order plus dead-time model is required
Specific software	Can support tuning an unsteady system	Higher cost

Table 3. Design parameters of the container ship.

Parameter	Value
Length	230.00 m
Beam	32.20 m
Draft	10.79 m
Displacement	57501 t
Block Coefficient	0.6742
Prismatic Coefficient	0.6832
Mid-ship Coefficient	0.9869
Water Plane Coefficient	0.8146

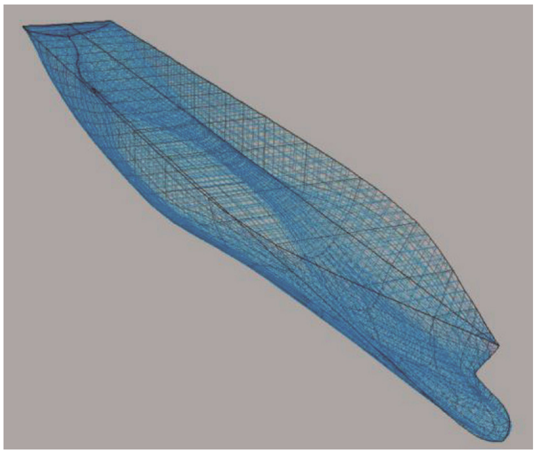

Fig. 5. Lines of the container ship.

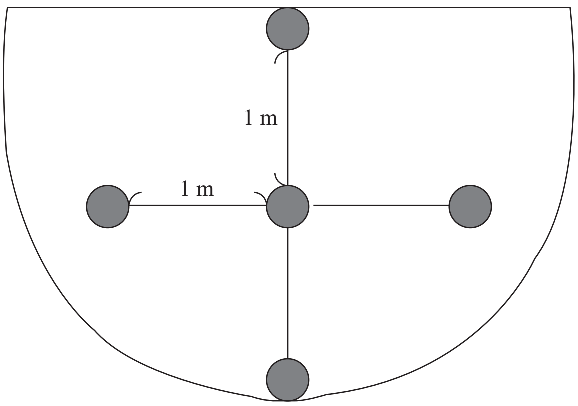

Fig. 6. Particle distribution of the container ship.

III. MODELING AND CONSTRUCTION OF MAPLE-SIM SYNCHRONIZATION SCHEMES

A multi-domain physical modeling software, MapleSim, is utilized to construct the system model of an ATARS in this study. Physical modeling combines mathematics with physical rules to describe a system constituted by single or multiple engineering elements. Because most engineering systems include corresponding dynamic characteristics, they can be defined using a dynamic differential equation. To solve the complex and difficult problem of water vehicles, which differ from traditional complex mathematical models, intuitive modeling is used to integrate the physical model and signal flow diagram into the simulation work environment. A controlled field model of the control system is established for the physical elements, and a closed-loop control signal flow is used to design the anti-rolling system. In addition, mathematical dynamic equations obtained through a derivation of the physical model can be used to introduce the definition of the algebraic constraints. To map a mathematical expression, it needs to be calculated using a solver in the software. This method can simulate the behavior of a ship for system identification to solve the transfer function and dynamic equation used by ATARS with high accuracy.

This paper adopts a container ship as the model, and the design parameters of which are listed in Table 3. A scaled down line diagram is utilized through a projection method, and repre-

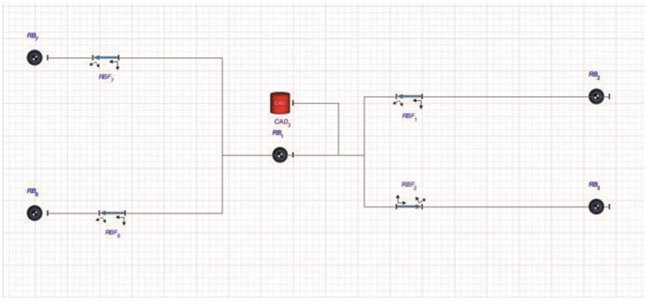

Fig. 7. A rigid model architecture diagram of a container ship model in MapleSim.

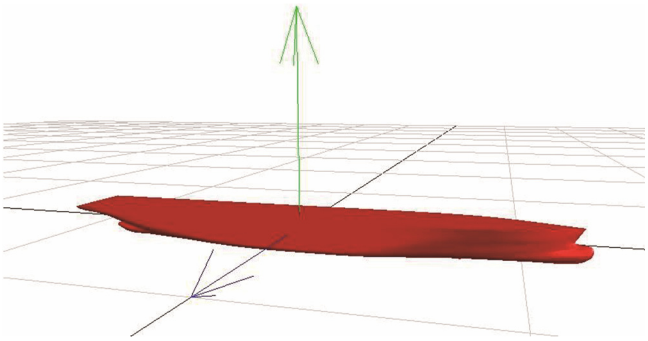

Fig. 8. A schematic diagram of a container ship model in a static state.

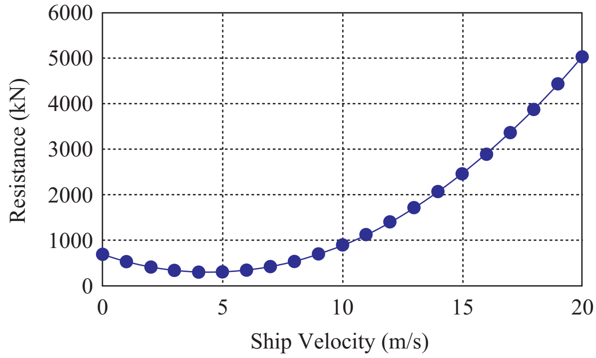

Fig. 9. Resistance curve of waves at various ship velocities.

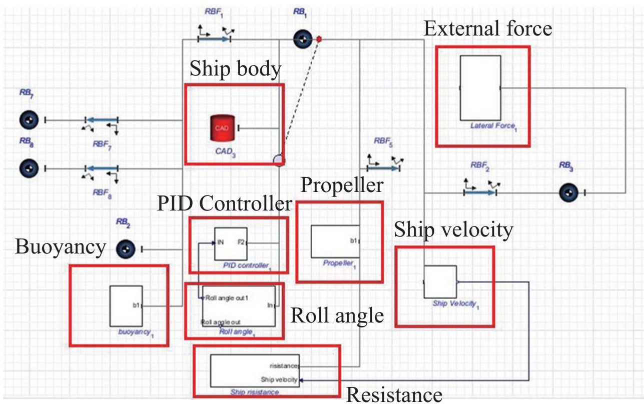

Fig. 10. Signal process architecture of forces and sensors in MapleSim.

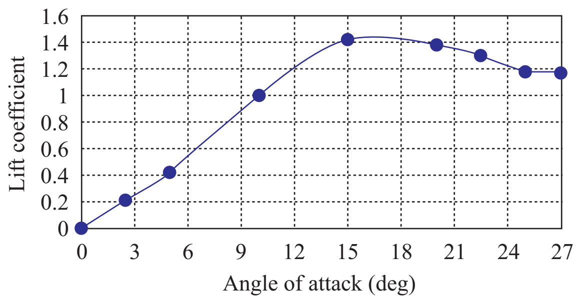

Fig. 11. Lift coefficient varying with different angles of attack.

sents the molded surface of the container ship. The 3D lines of the container ship are illustrated in Fig. 5.

The distance of the particle distribution marked in Fig. 6 has been revised. Big data on the actual distribution of mass were used. This study does not focus on how to divide a mesh, which should be simplified. An element (multi-body) in MapleSim can be imported drawing as a particle. If the entire container ship is treated as a particle, there is no roll motion. This study focuses on roll motion; therefore, the cross-section of the mid-ship is chosen, and divided into five particles with vertical and horizontal symmetry to represent the mass of the container ship. Five-article arrangement is shown in Fig. 6.

To import the container ship model into MapleSim, the container ship can be divided into an arrangement of five uniform particles, as shown in Fig. 6. A rigid model architecture diagram of a container ship model is shown in Fig. 7. Fig. 8 provides a schematic diagram of a container ship model, which is in a static state because it does not suffer from the influence of an external force.

To simulate a floating seaplane, buoyancy is added to the ship model. According to the commercial speed applied, thrust is needed to make the ship move forward. It should be noted that resistance is produced when the ship is sailing, which is relative to the ship velocity. The main reason for resistance is waves. Although wind may have an influence on the resistance, it is too weak to be considered. To obtain the resistance curve of the ship, the method developed by Hollenbach (1998) can be applied. A resistance curve from waves at various ship velocities is shown in Fig. 9.

To simulate the ship motion at sea, complex behaviors are required (Liang et al., 2013). Not only do hydrodynamic waves have complex boundary conditions, there are also six degrees of freedom in the ship motion. This paper investigates the effect of applying an ATARS, and to simplify the complex analysis in the flow fields, it treats the external force produced by beam sea as an equivalent transverse pulse. After creating the buoyancy, thrust, and transverse pulse, the signals of the forces and the sensors can be received in MapleSim to simulate harsh sea conditions for container ship at sea, as shown in Fig. 10.

In addition to the basic model, stabilizer fins need to be ad-

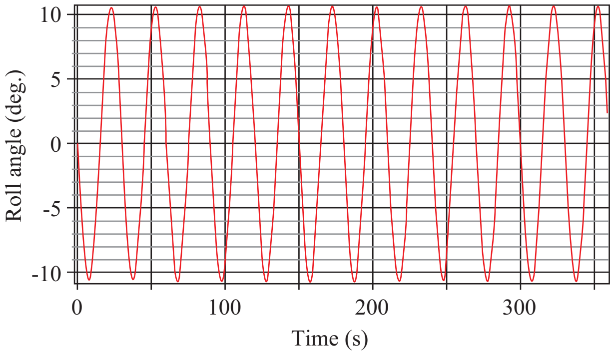

Fig. 12. Roll angle of container ship without ATARS.

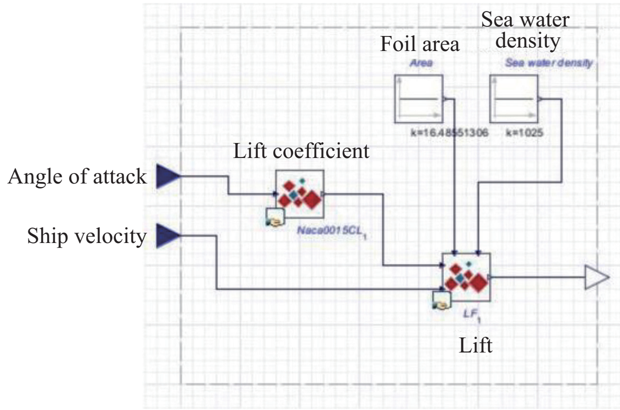

Fig. 13. Modeling framework of customized stabilizer fins in ATARS.

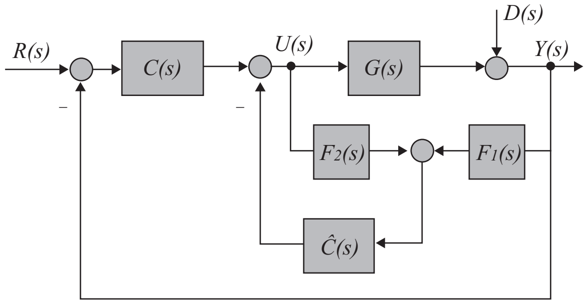

Fig. 14. System block diagram with modified PID controller.

ded as anti-rolling devices. The stabilizer fins generate lift, as estimated through Eq. (2). The density of sea water ρ is a constant, and the projected area S can be known based on Rhino CAD software. The velocity V is measured using the speed sensor in MapleSim. Fig. 11 shows that the lift coefficient C_L varies with different angles of attack (Subramanian et al., 2007). After rebuilding all of the forces mentioned above, the model is completed. The following two situations are compared in this study: one is a container ship without using an ATARS, and the other is a container ship using an ATARS with stabilizer fins.

IV. SIMULATION

1. Container Ship without ATARS

The container ship without an ATARS is used as the control group in the simulation, and can be the basis for improving the level of roll angle reduction as compared with the container ship with an ATARS. This paper divides the center of gravity into five particles with vertical and horizontal symmetry at the cross-section where the center of gravity is located. The container ship is in a stable forward state in calm waves.

To simulate the various roll motions created by the impact of the waves when the container ship is sailing, this paper considers a container ship hit by beam sea. To set up the external force perpendicular to the direction of the ship motion, sine waves instead of the beam sea are utilized in the simulation. The simulation continues for 360 s, the density of sea water is 1025 kg/m^3, the wave period is 30 s, the external force is 35,000 kN, and the ship velocity is 25 knots. Under these conditions, the simulated roll angle of a container ship without using an ATARS is shown in Fig. 12.

The period of roll motion is 30 s, and the range of roll angle is within ±10.6° when the container ship is hit by a sine wave with a period of 30 s. Clearly, it is unsuitable for sailors to operate under a roll angle of ±10°. A container ship without an ATARS has to react with different roll motions depending on the transvers force, which may cause the sailors to feel more discomfort when the ship is severely rolling.

2. Container Ship using ATARS with Stabilizer Fins

To add a pair of the stabilizer fins to both sides of a hull using an ATARS, a modeling framework of the customized stabilizer fin structure is applied, as shown in Fig. 13. The angle of attack is a constant if the system is a passive type. However, if the ATARS is an active type, it can find a suitable angle to change the righting moment using the designed PID controller. Using the relation between the angle of attack and the lift coefficient, the lift coefficient can be obtained. In addition, the projected area is affected by the angle of attack. Moreover, a velocity sensor is needed to obtain the speed. By combining the angles of attack, lift coefficients, projected area, and sea water density, the lift created using an ATARS with customized stabilizer fins can be calculated.

A modified PID controller, which refers to the design by Hagiwara is proposed to modify the angles of attack of the stabilizer fins used in an ATARS. The modified controller is different from a traditional PID controller in that it can specify the input-output characteristics and the disturbance attenuation characteristics separately and reduce unknown disturbances. A system block diagram including the modified PID controller is illustrated in Fig. 14.

In Fig. 14, $R(s)$ is the reference rolling input, $C(s)$ is the modified PID controller, $\hat{C}$ is the controller used to attenuate any unknown disturbances $D(s)$, and $F_1(s)$ and $F_2(s)$ indicate the signal procession.

Fig. 15 illustrates a flow chart of the active stabilizer fins designed for an ATARS. Fig. 16 shows the simulation results of the roll angle of the ship using the designed stabilizer fins.

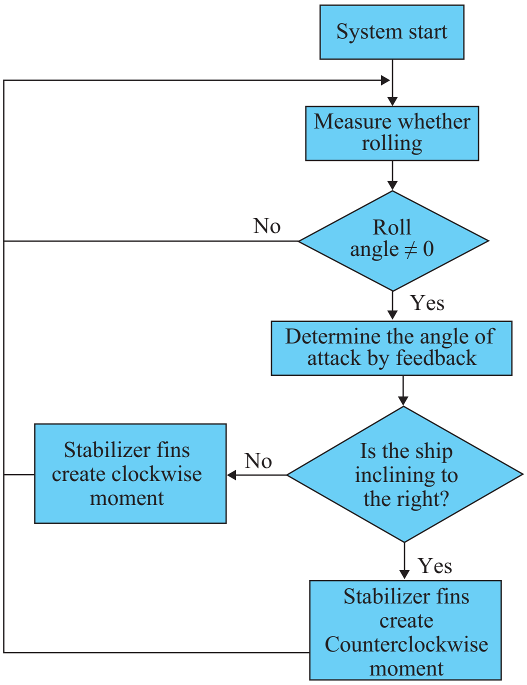

Fig. 15. Flow chart of active stabilizer fin design for use in ATARS.

Righting moment is created by the stabilizer fins applied against the roll motion of a container ship. Once the direction of the roll motion has changed, an opposite moment can be generated. This may cause the ship to shake for the duration of the moment. However, because the dimensions of a container ship larger than those of a human, a slight shaking may cause sailors to feel more physical discomfort when the ship is severely rolling.

The specifications of the roll angle of a container ship with stabilizer fins used in an ATARS can be observed; furthermore, the maximum overshoot is 5.1°, the settling time is 340 s, and steady-state error is 6.1°. The roll motion can converge to ±6.1° in 6 min, and the efficiency is defined as

$$\frac{R - R_a}{R} \times 100\% \qquad (6)$$

where R is the maximum absolute value of the roll angle without an ATARS, and R_a is the maximum absolute value of the roll angle of a container ship with an ATARS using stabilizer fins. Therefore, the efficiency is 42.45%.

V. CONCLUSION

The multi-domain physical modeling software, MapleSim, has many functions for solving dynamic problems. Not only does it make it easy to change the geometrical dimensions, it can also efficiently modify the controller parameters. Hence, it is a cost-effective and time-saving tool for a modeling design. This paper presented a simulation using MapleSim for considering the roll motion created by the impact of waves when a container ship is at sea. Based on the simulation results, it can be seen that the

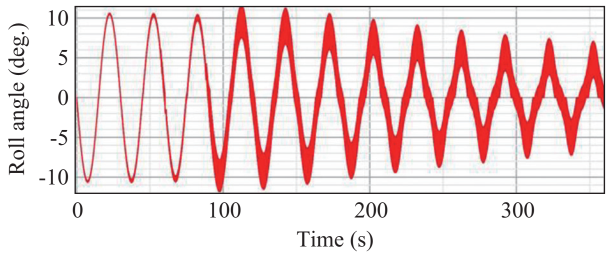

Fig. 16. Roll angle of the container ship with stabilizer fins used in ATARS.

roll motion of the a container ship without an ATARS is stable at ±10.6°. Under the same condition, the maximum overshoot, settling time, and steady-state error are 11.2°, 340 s, and 6.1°, respectively. The improvement is clear using a modified PID controller. The roll motion of a container ship with an ATARS using stabilizer fins can converge to ±6.1° in 6 min with an efficiency of 42.45 %.

REFERENCES

Ang, K. H., G. Chong and Y. Li (2005). PID control system analysis, design, and technology. IEEE Transactions on Control Systems Technology 13, 559-576.

Aziz, P. D. Abd., A. K. R. Mohanmad, F. Z. Hamidon, N. Mohamad, N. Salleh and N. Mohd Yunus (2014). A simulation study on airfoils using VAWT design for low wind speed application. Proceeding of 2014 4th International Conference on Engineering Technology and Technopreneuship (ICE2T), Kuala Lumpur, Malaysia, 105-109.

Datta, A., M. Z. Ho and S. P. Bhattacharyya (2000). Structure and synthesis of PID controllers, Springer Velag, London.

Hagiwara, T., K. Yamada, Y. Ando, I. Murakami, S. Aoyama and S. Matsuura (2010). A design method for modified PID control systems for multiple-input/multiple-output plants to attenuate unknown disturbances. Proceeding of 2010 World Automation Congress (WAC), Kobe, Japan, 1-6.

Hollenbach, K. U. (1998). Estimating resistance and propulsion for single-screw and twin-screw ships. Ship Technology Research 45, 72-76.

Kang, G. B., G. H. Chae and Y. B. Kim (2003). A study on system identification and anti-rolling system design of a ship with the flap. Proceeding of IEEE SICE 2003 Annual Conference, Fukui, Japan, 2294-2299.

Liang, L. H., B. H. Wang, S. T. Zhang and P. P. Xun (2013). Stabilizer fin effect on SWATH ship motions and disturbance observer based control design. Proceeding of 2013 IEEE International Conference on Mechatronics and Automation, Takamatsu, Kagawa, Japan, 1147-1152.

Liang, Y. H., K. Xue and H. Z. Jin (2009). Research on fin stabilizers with lift feedback employed multi-sensor data fusion technology., Proceeding of 2009 International Conference on Mechatronics and Automation, Changchun, China, 3070-3075.

Robert, J. B. (1982). A stochastic-theory for non-linear ship rolling in irregular seas. Journal of Ship Research 26, 229-245.

Subramanian, V. A., G. Asokumar and V. J. Kunar (2007). Active fin control for yacht using virtual instrumentation. Ocean Engineering, 34, 390-420.

Zhao, Y., M. Zhang, H. Chen. and X. F. Yuan (2014). Radar scattering from the composite ship-ocean scene: Doppler spectrum analysis based on the motion of six degrees of freedom. IEEE Transactions on Antennas and Propagation 62, 4341-4347.

Zhigang, Q., Y. Liu and J. Hong (2015). Research on the lift characteristic of morphing bionic fin stabilizer at zero/low speed. Proceeding of 2015 IEEE International Conference on Mechatronics and Automation (ICMA), Beijing, China, 1374-1378.

Zhong, J. (2011). PID controller tuning: a short tutorial. Purdue University.

Ziegler, J. G. and N. B. Nichols (1942). Optimum settings for automatic controllers. Transaction of the ASME 45, 759-768.